Available online at www.sciencedirect.com
ScienceDirect
Trans. Nonferrous Met. Soc. China 21(2011) 2049−2055
Transactions of Nonferrous Metals Society of China
www.tnmsc.cn

Triangular Au-Ag framework nanostructures prepared by multi-stage replacement and their spectral properties

YI Zao[1, 2], ZHANG Jian-bo[2], CHEN Yan[1, 2], CHEN Shan-jun[2, 3], LUO Jiang-shan[2], TANG Yong-jian[2, 3], WU Wei-dong[2], YI You-gen[1]

1. School of Physical Science and Technology, Central South University, Changsha 410083, China;
2. Research Center of Laser Fusion, China Academy of Engineering Physics, Mianyang 621900, China;
3. Institute of Atomic and Molecular Physics, Sichuan University, Chengdu 610065, China

Received 17 June 2010; accepted 15 August 2010

Abstract: Triangular Au-Ag framework nanostructures (TFN) were synthesized via a multi-step galvanic replacement reaction (MGRR) of single-crystalline triangular silver nanoplates in a chlorauric acid ($HAuCl_4$) solution at room temperature. The morphological, compositional, and crystal structural changes involved with reaction steps were analyzed by using transmission electron microscopy(TEM), energy-dispersive X-ray spectrometry (EDX), and X-ray diffraction. TEM combined with EDX and selected area electron diffraction confirmed the replacement of Ag with Au. The in-plane dipolar surface plasmon resonance (SPR) absorption band of the Ag nanoplates locating initially at around 700 nm gradually redshifted to 1 100 nm via a multi-stage replacement manner after 7 stages. The adding amount of $HAuCl_4$ per stage influenced the average redshift value per stage, thus enabled a fine tuning of the in-plane dipolar band. A proposed formation mechanism of the original Ag nanoplates developing pores while growing Au nanoparticles covering this underlying structure at more reaction steps was confirmed by exploiting surface-enhanced Raman scattering (SERS).

Key words: triangular Au-Ag framework nanostructures; multi-stage galvanic replacement reaction; surface plasmon resonance; surface-enhanced Raman scattering

1 Introduction

Recently, many scientists have interested in bimetallic nanostructures comprised of noble metals such as gold (Au), silver (Ag), platinum (Pt), and palladium (Pd) due to their fascinating optical [1], electronic [2], and catalytic [3] properties, leading to a wide range of applications, including SERS [4] and biosensors [5]. A variety of approaches for preparing bimetallic nano-materials have been investigated, including simultaneous chemical reduction of mixed metalions [6], photochemical method [7], and successive reduction of metal ions on the surface of sacrificial nanoparticles, also known as galvanic replacement reaction (GRR) [8−11]. Among them, as an effective and simple versatile tool, GRR has been extensively employed to synthesize bimetallic nanostructures in aqueous [12] or organic [13] media, such as hollow/porous [14] and core/shell particles [15].

Compared with one-step reaction approach, multi-step reaction is more favorable for composition and modality control. In this report, triangular Au-Ag framework nanostructures (TFN) were synthesized via a multi-step galvanic replacement reaction (MGRR) of single-crystalline triangular silver nanoplates in a chlorauric acid ($HAuCl_4$) solution at room temperature. Different reaction steps resulted in different morphologies, compositions, and crystal structures of the corresponding products, which were characterized by a series of techniques. And the growth mechanism as the MGRR unfolds was discussed.

2 Experimental

2.1 Synthesis of Ag nanoplates

Triangular Ag nanoplates were prepared by dual

Foundation item: Project (10804101) supported by the National Natural Science Foundation of China; Project (2007CB815102) supported by the National Basic Research Program of China; Project (2007B08007) supported by the Science and Technology Development Foundation of Chinese Academy of Engineering Physics, China
Corresponding author: YI You-gen; Tel: +86-816-2484233; E-mail: myyz1984@yahoo.cn
DOI: 10.1016/S1003-6326(11)60971-0

reduction method reported by MÉTRAUX and MIRKIN [16], of which the reaction mechanism has been investigated via careful spectroscopy characterization [17]. Generally, an appropriate amount of aqueous solution of $NaBH_4$ (0.1 mol/L) was injected with stirring into a aqueous mixture containing 50 mL $AgNO_3$ (0.1 mol/L), 3 mL trisodium citrate (30 mmol/L), 3 mL poly-(vinylpyrrolidone) (PVP, M_r=10000, 2 mmol/L) and 0.12 mL hydrogen peroxide (H_2O_2, w≈30%), and Ag nanoplate colloid with dark blue color was obtained after a series of color change.

2.2 Synthesis of gold-silver framework nanostructure

The as-prepared Ag colloid was continually stirred for 1 d to degrade the excess H_2O_2, and then it was treated according to multi-stage replacement strategy. In the replacement strategy, a constant amount of aqueous solution of $HAuCl_4$ (0.1 mmol/L) was added every half an hour into 10 mL Ag colloid. In both cases each addition was named one stage, and as the stages went on, the color of the colloid gradually changed from dark blue to light gray in the replacement case. All experiments were conducted at room temperature (23 °C) with constant stirring.

2.3 Instrumentation

A JEM−2010 transmission electron microscope (TEM) was used to observe the nanoparticles. All TEM samples were prepared by dropping the as-prepared colloids (centrifuged at 4 000 r/min for 30 min and then redispersed in 2 mL de-ionized water) on copper grids and drying in air. Energy dispersive X-ray spectra (EDX) were recorded on an Oxford INCA energy spectroscope. X-ray diffraction patterns (XRD) were recorded on an X'Pert PRO X-ray diffractometer using Cu K_α (40 kV, 40 mA) radiation. All XRD samples were prepared by dropping some centrifuged colloid on clean glass slides and drying. All UV-Vis-NIR spectra were recorded within a quartz cell of 1 cm optical length on a Perkin-Elmer Lambda 12 spectrophotometer.

R6G solution was diluted to 1×10^{-6} mol/L with water, and then 20 μL solution was dropped into the quartz cuvette with an optical path of 1 cm using 1 mL colloid product. Raman spectra were obtained with a Renishaw 2000 model confocal microscopy Raman spectrometer with a CCD detector and a holographic notch filter (Renishaw Ltd, Gloucestershire, U.K.). The microscope attachment was based on a Leica DMLM system, and an objective was used to focus the laser beam onto a spot with approximately 1 μm in diameter. Radiation of 514.5 nm from an air cooled argon ion laser (Spectra-Physics Model 163−C4260) was used for excitation. All of the spectra reported were the results of a single accumulation of 20 s.

3 Results and discussion

3.1 TEM images

TEM images of the initial Ag nanoparticles and their sequent derivatives after multi-stage replacement are shown in Fig. 1. Majority of the initial particles obtained by dual reduction method were in shape of triangle with mild outlines, and their average edge length was measured to be (35±8) nm (Fig. 1(a)). The inset of Fig. 1(a) shows the close stacking of several nanoplates with their lateral sides upward, enabling to estimate the thickness of these nanoplates to be about 5.3 nm. Figure 1(b) shows the selected-area electron diffraction (ED) pattern of one flat-lying nanoplate with its top surface perpendicular to the electron beam, in which the spots enclosed in the rectangle, triangle and circle correspond to the {220}, {422} and 1/3{422} Bragg reflections of face-centered cubic (fcc) silver, respectively. The existence of {220} reflection indicates that the nanoplates were single crystals with {111} planes as the basal planes, and the appearance of normally forbidden 1/3{422} reflection implies the presence of number of (111) stacking faults lying parallel to the {111} surface and extending across the entire nanoplate [18]. Thus, it is reasonable that the top and bottom surfaces of the nanoplates are bounded by atomically flat {111} planes[19]. Figures 1(c)−(f) show the TEM images of the products after 1, 3, 5 and 7 stages of replacement of Ag nanoplates with $HAuCl_4$. The nanoplates kept solid surface after 1 stage (Fig. 1(c)), but some plates after 3 stages already took on void areas on their planar surfaces (Fig. 1(d)). As stages increased, the percentage of plates having void area increased and the void area enlarged (Fig. 1(e)). After 7 stages most plates changed into triangular nanorings of which central parts were almost hollow (Fig. 1(f)). The four particles stacking together with their lateral sides upward in the inset of Fig. 1(f) clearly show that although the flat {111} facets of Ag nanoplates had visible void zones after 7 stages, their lateral sides still kept intact with no apertures at all. In addition, ED pattern of the nanorings in Fig. 1(f) was also recorded (omitted here), which revealed the single crystal fcc essence of the TFN.

3.2 XRD patterns of products

Figure 2 shows the XRD patterns of Ag nanoplates and products after 3 and 7 stages of replacement. The four distinct peaks in pattern of Ag nanoplates are assigned to diffraction from {111}, {200}, {220} and {311} planes of single-crystalline fcc silver, respectively. This accords with the result of ED pattern. While in the

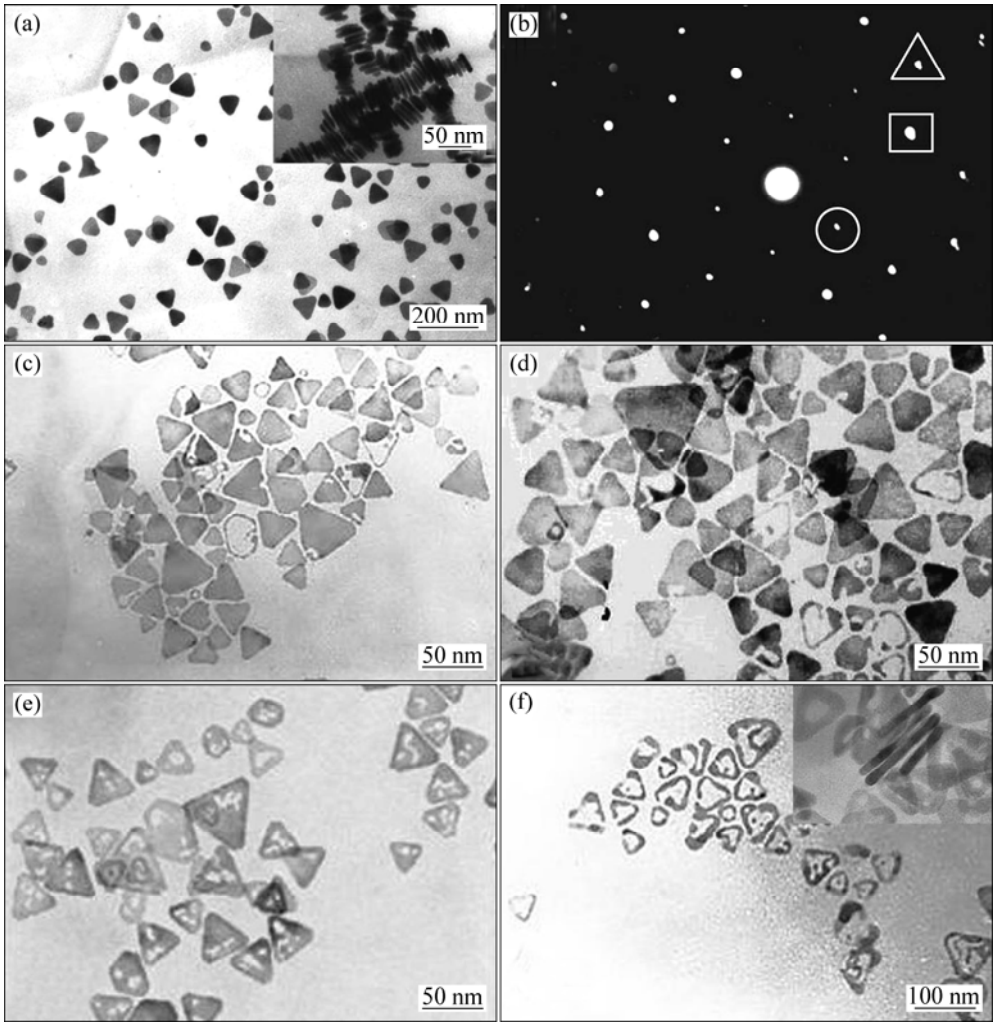

Fig. 1 TEM images of initial Ag nanoplates and products after multi-stage replacement: (a) Initial Ag nanoplates; (b) ED pattern of single nanoplate in (a); (c)-(f) Products after 1, 3, 5 and 7 stages, respectively

patterns of both replaced products, the originally strongest (111) peak became indistinguishable, which occurred as a result of the gradual loss of {111} facets of the Ag plates by etching during the replacement process, as displayed in the TEM images. Here the several peaks within 35°−45° might be caused by the glass slide substrate, and they were invisible in the pattern of initial Ag nanoplates just because they were too weak compared with the strong Ag (111) peak.

3.3 EDX patterns

To examine the composition of the structures, EDX measurements were also performed. EDX spectra of initial Ag nanoplates and Au-Ag framework nanostructures obtained after 7 stages of replacement were recorded as shown in Fig. 3, which confirmed that the initial plates consisted of pure silver, and the final Au-Ag rings consisted of both silver and gold (the copper element came from the copper grids). The coexistence of silver and gold in the void rings means that the replacement stages could be increased more to bring more $HAuCl_4$ to completely substitute silver.

3.4 UV-Vis absorption spectra of products

A UV-Visible spectrophotometer is a very convenient tool for monitoring the evolution of metal nanoparticles in solution-phase, due to their specific surface plasmon resonance (SPR) excitation of various morphologies. SPR is an optical phenomenon which occurs in the interaction of electrons of metal nanoparticles. As the surface plasmon resonance (SPR) absorption of metal nanoparticles like gold and silver is very sensitive to the changes of the size and shape, this sensitivity could be used as a tool to monitor the shape of the particles through the optical extinction spectrum. The photograph and absorption spectra of products after multi-stage replacement are shown in Fig. 4. Figure 4(a) shows the color change of products. The color of the colloid gradually changed from dark to light gray. Figure 4(b) shows the absorption spectra of products. The initial

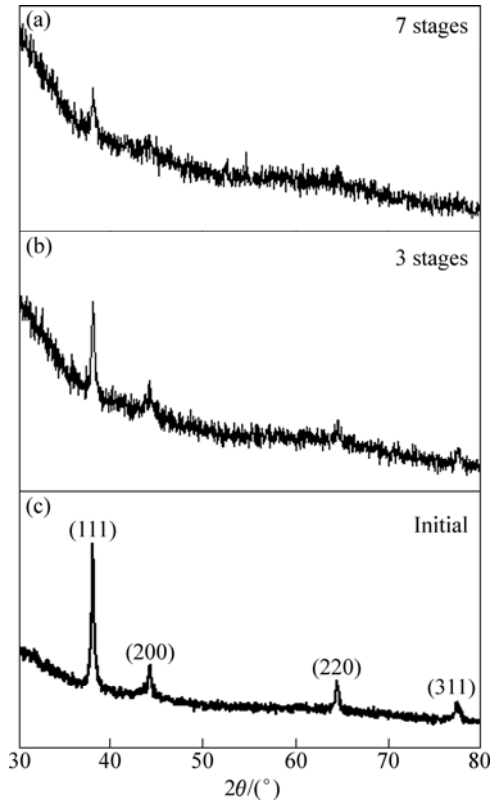

Fig. 2 XRD patterns of Ag nanoplates and products after 3 and 7 stages of replacement

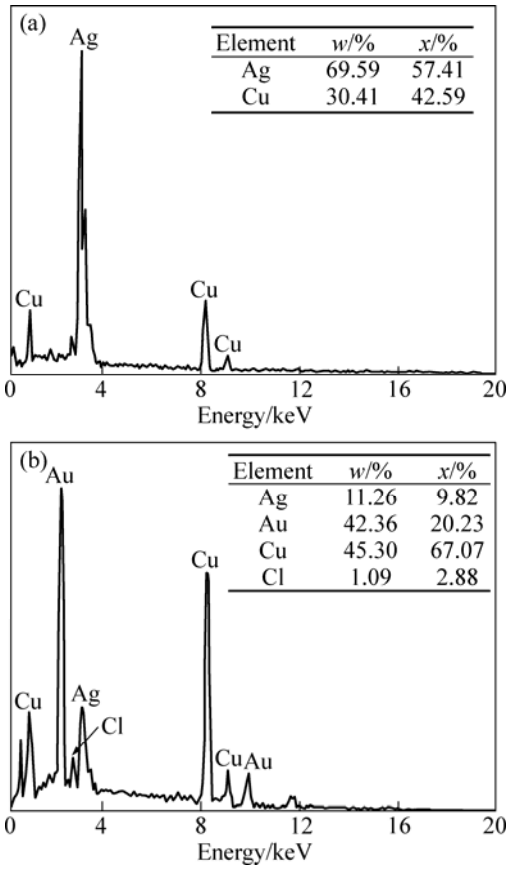

Fig. 3 EDX spectra of initial Ag nanoplates (a) and Au-Ag framework nanostructures after 7 stages of replacement (b)

Ag nanoplates exhibited three peaks: a small peak at 332 nm, a shoulder peak at 470 nm, and a strong peak at 708 nm, which can be ascribed to the out-of-plane quadrupolar, in-plane quadrupolar and in-plane dipolar SPR absorption band of Ag nanoplates, respectively [20]. The in-plane dipolar band is always paid more attention to, as it holds the strongest peak and is the most sensitive to change of the anisotropy and component of the nanoplates. Figure 4(b) reveals that during the multi-stage replacement, the out-of-plane quadrupolar band hardly shifted, the in-plane quadrupolar band redshifted slightly within 100 nm, and the in-plane dipolar band redshifted from around 700 nm to near 1 100 nm step by step, entering the near infrared region. The production of out-of-plane quadrupolar band is related with the lateral sides of nanoplates of electron oscillation. Because the lateral sides of Au-Ag framework nanoplates still kept intact with no holes at all [20], so the out-of-plane quadrupolar band hardly shifted. However, the production of in-plane quadrupolar and in-plane dipolar SPR absorption band is related with the bottom flat facets of nanoplates of electron oscillation. This shift arose from the deposition of Au atoms onto Ag templates and the subsequent etching, which caused appearance of holes and finally led to void nanorings with thin walls. It is the holes that played an important role in leading the SPR band of metal nanostructures shift into long waveband [10, 21].

Comparison experiments of changing the quantity of $HAuCl_4$ added per stage were conducted, and the redshift results are listed in Table 1, which show that

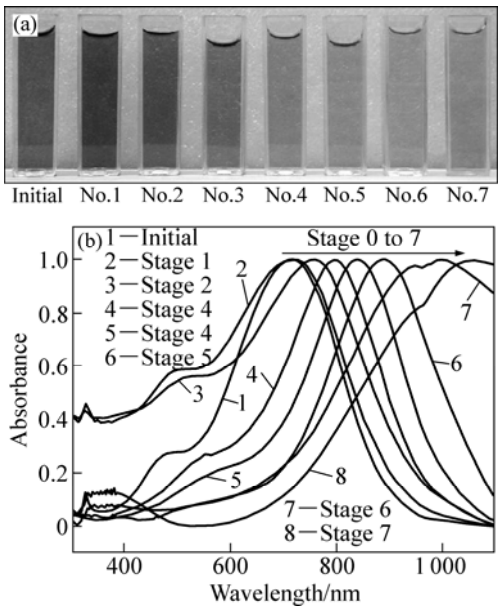

Fig. 4 Photograph (a) and absorption spectra (b) of products after multi-stage replacement (0.2 mL 0.1 mmol/L $HAuCl_4$ was added into 10 mL Ag colloid per stage, all spectra were normalized against intensities of the strongest peaks.)

adding 0.1, 0.2 or 0.3 mL $HAuCl_4$ per stage led to 100, 295 or 81 nm redshift of the in-plane dipolar band after 7 stages, respectively. This implies that a further fine tuning of the SPR band can be easily accomplished by elaborately tuning the adding amount of Au precursor per stage.

Table 1 Redshift of in-plane dipolar peak of products with different adding amount of $HAuCl_4$ per stage during multi-stage replacement

Adding amount of 0.1 mmol/L $HAuCl_4$ per stage/mL	Initial in-plane dipolar peak/nm	Stage number	Total redshift/ nm	Average redshift per stage/nm
0.1	700	7	100	13
0.2	700	7	295	37
0.3	700	7	81	10

3.5 SERS spectra

To further confirm the suggested process, one can employ SERS measurements of the various nanostructures. We used Rhodamine 6G as the probe molecules and the 514.5 nm line of an argon laser as excitation, to ensure that the SERS effects are sensitive only to the Ag yet still strong with little Ag present. Au is completely unresponsive to this excitation because its nanostructures' plasmon resonances are well-known to be further in the red wavelengths. In this way, one can monitor the covering of the Ag by the Au. We chose Rhodamine 6G as the probe molecule because of its large Raman cross section, leading to strong SERS signals even if the Au has already replaced much of the Ag substrate [22]. Figure 5(a) shows the result when using water, for the sake of comparison. It is a featureless spectrum at the resolution chosen. Figures 5(b)−(f) show the spectra of R6G adsorbed on initial Ag nanoparticles before MGRR (0 stage) and after MGRR with $AuCl_4^-$ for 1, 3, 5, and 7 stages, respectively. Several strong bands at 1 651, 1 599, 1 574, 1 508, 1 362, 1 310, 1 188, 775 and 612 cm^{-1} are observed on the curves. The bands at 1 651, 1 574, 1 508 and 1 362 cm^{-1} are assigned to aromatic C—C stretching; 1 599 and 1 126 cm^{-1} are assigned to C═C stretching; 1 188 cm^{-1} is assigned to aromatic C—H bending; 612 cm^{-1} is assigned to aromatic bending, respectively [23]. From the four right bars comparing the plateau with the strongest peak in the intensity (aromatic C—C stretching at ca. 1 651 cm^{-1}) in curves (b)−(f), we find that the Raman enhancements by the samples after 1 (26 330 units) and 3 (9 846 units) stages are both greater than pure Ag nanoplates, although the SERS effectiveness of Ag is usually better than that of Au or as-investigated alloys [24]. This SERS enhancement may be related to several factors. First, surfaces of bimetals provide more possibilities for molecules to deposit on the boundaries between Ag and Au domains [25]. Second, adequate amounts of Au in a homogeneous alloy (solid solution) may intrinsically enhance the SERS activity. However, since the intrinsic activity of Ag is much higher [26], the most important reason may not be related to the added Au directly, but rather the corresponding morphological change of the underlying Ag nanoplates. The MGRR leaves pores where Ag is depleted. High-curvature features can cause very large enhancement (lightening rod effect) for molecules adsorbed on the tips of needles or on edges [27].

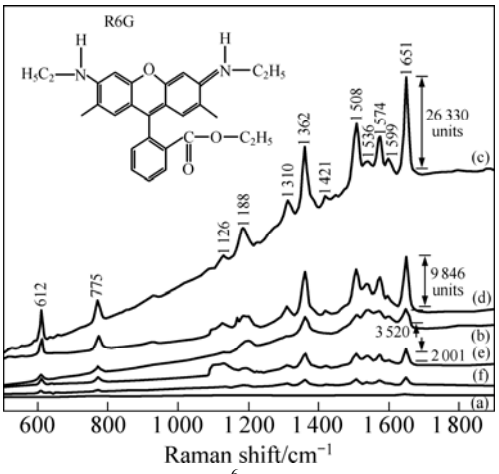

Fig. 5 Raman spectra of 10^{-6} mol/L R6G into bare water (a) and initial Ag nanoplates (b) and Ag-Au nanostructures (c−f) (1, 3, 5 and 7 stages, respectively)

Two close metallic surfaces can enhance the electromagnetic (EM) field around molecules absorbed between them, which leads to SERS enhancement [28]. However, as the MGRR stages increase from 5 to mores, SERS enhancement again decreases. This confirms the increase in SERS-inactive Au covering active Ag. As shown in curves (e) (2 001 units) and (f) from Fig. 5, their SERS enhancement is much below that of the initial unmodified Ag nanoplates. First, compared with the 3 stages-sample, the content of the SERS inert Au increases further. Again, this may be due to complex alloy surface chemistry or in the case of MGRR due to the fact that deposited Au increasingly starts to change and even more simply hide the rough SERS active Ag structure beneath. By investigating the SERS behavior, we can employ it to monitor how Au covers Ag as the MGRR unfolds.

3.6 Analysis of mechanism

Galvanic replacement reaction has been demonstrated as a general and effective means for preparing metallic nanostructures by consuming the more reactive component. Since the standard reduction

potential of $AuCl_4^-$/Au pair (0.99 V vs standard hydrogen electrode, SHE) is higher than that of the Ag^+/Ag pair (0.80 V vs SHE), silver would be oxidized into Ag^+ when silver nanostructures and $HAuCl_4$ are mixed in an aqueous medium.

$$3Ag(s)+AuCl_4^-(aq) \rightarrow Au(s)+3AgCl(s)+Cl^-(aq)$$

The oxidation of Ag^0 into Ag^+ leads to the gradual consumption of Ag, at the same time, the production of Au^0, which is deposited on the Ag nanoplates.

According to the previous reports, the above phenomena can be explained as follows. The free energies of three crystalline planes of an fcc metal rank in such order: $\gamma\{110\}>\gamma\{100\}>\gamma\{111\}$ [29]. When Ag nanoplates reacted with $HAuCl_4$, the replacement initiated from the edge facets (mainly bounded by {110} or {100} planes) of the nanoplates rather than the top and bottom flat facets (bounded by the most stable {111} plane), thus led to quick formation of a Au framework around the edges [30]. As the nanoplates had lateral thickness less than 10 nm, reaction against the {111} facets could not generate complete Au shell to construct two continuous {111} planes according to report of ZOU et al [27]. The replaced Au atoms deposited onto Ag as a thin layer, but they were so unstable that they dissolved into the solvent and reconstructed via processes such as Ostwald ripening to grow onto the lateral Au framework [31], thus void nanorings formed. As Au and Ag have almost the same lattice constant, it is easy for them to coexist in alloy [32], therefore the replaced void structures were made up of single-crystalline Au-Ag framework nanostructures [33].

4 Conclusions

1) Triangular Au-Ag framework nanostructures were synthesized via a multi-stage galvanic replacement reaction (MGRR) of single-crystalline triangular silver nanoplates in a chlorauric acid ($HAuCl_4$) solution at room temperature. Different reaction steps resulted in different morphologies, compositions, and crystal structures of the corresponding products.

2) The in-plane dipolar surface plasmon resonance (SPR) absorption band of the Ag nanoplates locating initially at around 700 nm gradually redshifted to 1 100 nm via a multi-stage replacement after 7 stages. The adding amount of $HAuCl_4$ per stage influenced the average redshift value per stage, thus enabled a fine tuning of the in-plane dipolar band. By investigating the SERS behavior, we can employ it to monitor how Au covers Ag as the MGRR unfolds. Compared with one-step replacement, multi-stage galvanic replacement reaction is more favorable for composition and modality control. The MGRR was found to play a critical role in forming uniform TFN.

References

[1] WU W T, ZHOU T, ZHOU S Q. Tunable photoluminescence of ag nanocrystals in multiple-sensitive hybrid microgels [J]. Chem Mater 2009, 21(13): 2851−2861.

[2] VAMSI K K, GUO W H, XIAO M. Surface plasmon density of states at the metal-dielectric interface: Dependence of metal layer thickness and dielectric material [J]. J Appl Phys, 2010, 107(6): 1−5.

[3] YASUO L, TOMONOBU M, TAKUMI M, MITSUTAKA O, MASAKAZU D, MASATAKE H. A kinetic study on the low temperature oxidation of CO over Ag-contaminated Au fine powder [J]. Journal of Catalysis, 2009, 262(3): 280−286.

[4] KWAN K, KYUNG L K, CHOI J Y, LEE H B, SHIN K S. Surface enrichment of Ag atoms in Au/Ag alloy nanoparticles revealed by surface-enhanced Raman scattering of 2,6-dimethylphenyl isocyanide [J]. J Phys Chem C, 2010, 114(8): 3448−3453.

[5] WANG L Y, SUN Y, WANG J, ZHU X N, JIA F, CAO Y B, WANG X H, ZHANG H Q, SONG D Q. Sensitivity enhancement of SPR biosensor with silver mirror reaction on the Ag/Au film [J]. Talanta, 2009, 78(4): 265−269.

[6] LINK S, WANG Z L, EL M A. Alloy formation of gold-silver nanoparticles and the dependence of the plasmon absorption on their composition [J]. J Phys Chem B, 1999, 103(19): 3529−3533.

[7] TREGUER M, COINTET C D, REMITA H, KHATOURI J, MOSTAFAVI M, AMBLARD J, BELLONI J. Dose rate effects on radiolytic synthesis of gold-silver bimetallic clusters in solution [J]. J Phys Chem B, 1998, 102(22): 4310−4321.

[8] WANG S R, HE J A, XIE J L, ZHU Y X, XIE Y C. Synthesis of bimetallic systems using replacement reactions [J]. Applied Surface Science, 2008, 254(6): 2102−2109.

[9] NING Xiao-hua, XU Shu-ping, DONG Feng-xia, AN Jing, TANG Bin, ZHOU Ji, XU Wei-qing. Gold-silver framework monolayer nanostructure prepared by in-situ sacrificial template reaction and their application for SERS [J]. Chemical Journal of Chinese Universities, 2009, 30(1): 159−163. (in Chinese)

[10] ZOU X Q, YING E B, DONG S J. Preparation of novel silver–gold bimetallic nanostructures by seeding with silver nanoplates and application in surface-enhanced Raman scattering [J]. Journal of Colloid and Interface Science, 2007, 306(3): 307−315.

[11] DAMIAN A, MATTEW G, JOHN M K, YURII K G. From Ag nanoprisms to triangular AuAg nanoboxes [J]. Adv Funct Mater, 2010, 20(6): 1329−1338.

[12] SUN Y G. Conversion of Ag nanowires to AgCl nanowires decorated with Au nanoparticles and their photocatalytic activity [J]. J Phys Chem C, 2010, 114 (5): 2127−2133.

[13] YANG J, LEE J Y, TOO H P. A. Bis (p-sulfonatophenyl) phenylphosphine-based synthesis of hollow Pt nanospheres [J]. J Phys Chem B, 2006, 110(1): 125−129.

[14] JIN Y D, DONG S J. One-pot synthesis and characterization of novel silver-gold bimetallic nanostructures with hollow interiors and bearing nanospikes [J]. J Phys Chem B, 2003, 107(47): 12902−12905.

[15] DAVID B, WANG SH L, SCOTT E J, LIANG H. Adsorbate-induced diffusion of Ag and Au atoms out of the cores of Ag@Au, Au@Ag, and Ag@AgI core-shell nanoparticles [J]. J Phys Chem C, 2007, 111(37): 13665−13672.

[16] METRAUX G S, MIRKIN C A. Rapid thermal synthesis of silver nanoprisms with chemically tailorable thickness [J]. Adv Mater, 2005, 17(4): 412−415.

[17] GUO Bing, TANG Yong-jian, LUO Jing-shan. Study on absorption and emissionspectroscopy of triangular silver nanoplates prepared by

dualreduction method [J]. Precious Metals, 2008, 29(2): 5−10. (in Chinese)
[18] CHEN S, CARROLL D L. Silver nanoplates: Size control in two dimensions and formation mechanisms [J]. J Phys Chem B, 2004, 108(18): 5500−5506.
[19] JIN R, CAO Y, MIRKIN C A. Photoinduced conversion of silver nanospheres to nanoprisms [J]. Science, 2001, 294: 1901−1903.
[20] KELLY K L, CORONADO E, ZHAO L L. The optical properties of metal nanoparticles: the influence of size, shape, and dielectric environment [J]. J Phys Chem B, 2003, 107(3): 668−677.
[21] SUN Y, MAYERS B, XIA Y. Metal nanostructues with hollow interiors [J]. Adv Mater, 2003, 15(7−8): 641−646.
[22] KEATING C D, KOVALESKI K K, NATAN M J. Heightened electromagnetic fields between metal nanoparticles: Surface enhanced Raman scattering from metal-cytochrome c-metal sandwiches [J]. J Phys Chem B, 1998, 102(8): 9414−9425.
[23] WEI G, ZHOU H L, LIU Z G. A simple method for the preparation of ultrahigh sensitivity surface enhanced Raman scattering (SERS) active substrate [J]. Applied Surface Science, 2005, 240(4): 260−267.
[24] RIVAS L, SANCHEN S, GARCIA J, MORCILLO G. Alloy formation of gold-silver nanoparticles and the dependence of the plasmon absorption on their composition [J]. Langmuir, 2000, 16(12): 9722−9728.
[25] LIU Y C, YANG S J. Improved surface-enhanced Raman scattering based on Ag-Au bimerials prepared by galvanic replacement reactions [J]. Electrochim Acta, 2007, 52(5): 1925−1931.
[26] FREEMAN R G, HOMMER M B, GRABAR K C, JACKSON M A, NATAN M J. Ag-clad Au nanoparticles: novel aggregation, optical, and surface-enhanced raman scattering properties [J]. J Phys Chem, 1996, 100(2): 718−724.
[27] ZOU X Q, YING E B, DONG S J. Preparation of navel silver-gold bimetallic nanostructure by seeding with silver nanoplates anf application in surface-enhanced raman scattering [J]. J Colloid Interface Sci, 2007, 306(1): 307−315.
[28] LIVER N, NITZAN A, GERSTEN J. Local fields in cavity sites of rough dielectvic surfaces [J]. J Chem Phys Lett, 1984, 111(4): 449−454.
[29] WANG Z L. Transmission electron microscopy of shape controlled nanocrystals and their assemblies [J]. J Phys Chem B, 2000, 104(6): 1153−1175.
[30] SUN Y, MAYERS B, XIAY N. Metal nanostructues with hollow interiors [J]. Adv Mater, 2003, 15(7−8): 641−646.
[31] JIANG L, XU S, ZHU J. Ultrasonic-assisted synthesis of monodisperse single-crystalline silver nanoplates and gold nanorings [J]. Inorg Chem, 2004, 43(19): 5877−5883.
[32] NING Yuan-tao. Development and progress of gold and gold alloy materials [J]. Precious Metals, 2007, 28(2): 57−64. (in Chinese)
[33] SUN Y, XIA Y. Alloying and dealloying processes involved in the preparation of metal nanoshells through a galvanic replacement reaction [J]. Nano Lett, 2003, 3(11): 1569−1572.

多轮置换法制备的 Au-Ag 三角纳米环及其光学性能

易 早[1,2]，张建波[2]，陈 艳[1,2]，陈善俊[2,3]，罗江山[2]，唐永建[2,3]，吴卫东[2]，易有根[1]

1. 中南大学 物理科学与技术学院，长沙 410083；
2. 中国工程物理研究院 激光聚变研究中心，绵阳 621900；
3. 四川大学 原子与分子物理研究所，成都 610065

摘 要：以双还原剂法制备的单晶三角形银纳米盘为模板，在室温 $HAuCl_4$ 溶液中发生多轮置换反应，制备 Au-Ag 三角纳米环材料。采用 TEM、EDX 和 XRD 等检测手段表征反应阶段产物的形貌、组成以及晶体结构。TEM、EDX 和电子衍射谱证实 Au 置换了 Ag。反应 7 轮后纳米盘的面内偶极表面等离子体共振峰从初始的 700 nm 逐步红移到 1100 nm，形貌从实心盘状逐渐变为空心纳米环。改变每轮加入的 $HAuCl_4$ 量即可精细调节面内偶极峰的红移步进量。通过采用 SERS 光谱检测方法，随着多步置换反应的进行，提出了一个可行的形成机理机制。

关键词：Au-Ag 三角纳米环；多轮置换反应；表面等离子体共振；表面增强拉曼光谱

(Edited by LI Xiang-qun)